



# Potential of the KOBO extrusion process for nonferrous metals in the form of solids and chips

Włodzimierz Bochniak<sup>1</sup> · Paweł Ostachowski<sup>1</sup> · Andrzej Korbel<sup>1</sup> · Marek Łagoda<sup>2</sup>

Received: 12 December 2022 / Accepted: 12 May 2023 / Published online: 18 May 2023  
© The Author(s) 2023

## Abstract

The research undertaken for this paper was inspired by the results of theoretical analyzes and strong experimental evidence confirming the possibility to induce the phenomenon of viscous flow (typical for liquids) in the process of low-temperature KOBO extrusion of metals. Thus, despite the constant solid state of the metal, the KOBO plastic deformation process requires much lower stress (low flow resistance) in comparison with conventional extrusion. On the other hand, the KOBO method is particularly attractive due to the generation of high strength properties in the product/extrudate favorable for low (room) temperature deformation as well as superplastic features at higher temperature ranges.

This paper presents the results of the studies on the efficiency of low-temperature KOBO extrusion of hardly-deformable materials in massive form (Mg4Li, AK11, Cu6.5P) and fragmented fractions (2014, 7075, AZ91, titanium grade 2). Particular attention was paid to the structure and mechanical properties of the obtained extrudates, which were rated as exceedingly favorable. As such, the paper provides new technological arguments for the application of the KOBO method in plastic deformation of materials as it guarantees their functional properties.

**Keywords** Nonferrous metals · Ingot · Chips · KOBO extrusion · Structure · Mechanical properties

## 1 Introduction

In earlier paper by Korbel [1] it was established that viscous flow is the dominant deformation mechanism in the KOBO extrusion of metals and it can be described by a linear mechanical characteristic typical for liquids and defined as Newtonian laminar flow:

$$\sigma = \eta \cdot \dot{\epsilon} \quad (1)$$

(where  $\sigma$  – flow stress,  $\eta$  – viscosity coefficient,  $\dot{\epsilon}$  – strain rate).

Proving this relationship to be true during low-temperature metal deformation is undoubtedly an important scientific discovery and should inspire further research of the phenomenon itself and its technological aspects (metal forming technology).

The description of the KOBO method, which gives the metal particular structural state responsible for the viscous flow phenomenon, together with an attempt at explaining its physical background can be found in papers [1, 2]. The results presented in this paper are based on the knowledge on the deformation mechanism and ways of controlling it, and focus mainly on the assessment of practical possibilities to impact the structure and mechanical properties of non-ferrous metal alloys in massive and fragmented form by KOBO extrusion.

Firstly, it is necessary to outline the distinctive features of the KOBO method and list the structural elements generated during its application as well as their relationships with the deformation mechanism and mechanical characteristics of the process. The KOBO extrusion process involves reverse twisting of the die in order to create an additional simultaneous reverse twist of the metal, i.e., conditions for permanent change of deformation path. In comparison with conventional extrusion, the KOBO method involves two new parameters, namely the angle and frequency of twisting. As a result, an intense localized plastic deformation – stratified flow [3], occurs and an enormous, overequilibrium concentration of point defects, particularly self-interstitial atoms

✉ Paweł Ostachowski  
pawel.ostachowski@agh.edu.pl

<sup>1</sup> Faculty of Non-Ferrous Metals, AGH – University of Science and Technology, A. Mickiewicza Av. 30, 30–059 Cracow, Poland

<sup>2</sup> Łukasiewicz Research Network – Institute of Non-Ferrous Metals, Sowińskiego St. 5, 44–100 Gliwice, Poland

with unusually low migration energy (e.g. of around 0.06 eV for aluminum) is generated [1]. This leads to a significant drop in the strength of bonds in the crystal lattice, which lowers the metal's viscosity coefficient value to the level observed in liquids ( $10^8$  Pa·s) and creates the conditions for the dominance of stratified flow. The phenomenon is accompanied by a drop in plastic flow resistance, as shear resistance in the viscous layers is very low. Therefore, even though the deformed metal constantly remains in a solid state, it behaves similar to a liquid and at low (e.g., room) temperatures can reach a very high extrusion ratio  $\lambda$  without the need to limit the speed [3] of the process (strain rate).

What is particularly attractive about the KOBO method is that the concentration of point defects remains high in the final product/extrudate as well. At low temperatures it results in high strength properties and at higher temperatures and low strain rate it allows for the metal to reach a superplastic state similar to the one occurring during KOBO process.

Transmission electron microscopy (TEM) observations of pure metal revealed [3] that after the KOBO process it contains densely situated nanometric clusters of point defects, mainly self-interstitial atoms. Such formation of point defects must have been created during or immediately after the KOBO extrusion (post-deformation effect). It is important to point out that the diffusion coefficient  $D$  indicated for the metal undergoing KOBO extrusion is by several dozen levels of magnitude higher than the equilibrium value.

$$D = D_0 \cdot c_d \cdot \exp\left(\frac{-E_d}{k \cdot T}\right) \quad (2)$$

(where:  $D_0$  – constant: geometrical and frequency parameter,  $c_d$  – concentration of self-interstitial atoms,  $E_d$  – migration energy of self-interstitial atoms,  $k$  – Boltzmann constant,  $T$  – absolute temperature).

Similar to the role of second phase particles in alloys, point defect clusters are an obstacle to deformation via

dislocation slip by raising the material's strength properties. On the other hand, clusters can be transformed („dissolved”) into many separate point defects, thus „oversaturating” the metal as a result of both – the effect of heat (high temperature) and the applied deformation. In both cases localized stratified flow, albeit of different intensity, can be observed.

This paper presents the results of experimental research on low-temperature KOBO extrusion of hardly-deformable non-ferrous metallic (mainly light) materials (Tables 1 and 2). The samples were either in the form of massive (ingots from the AK11, Mg4Li and Cu6.5P alloys) or fragmented (chips from the 2014, 7075, AZ91 and Ti Grade 2 materials) and differed in terms of strengthening state (after casting, after heat- and mechanical- treatments).

Particular attention was paid to the studies of extrudates/products which were subjected to structural observations and strength testing (tensile tests at room temperature).

## 2 Methodology

The KOBO extrusion process was carried out on a horizontal laboratory hydraulic press with a maximum force of 1100 kN equipped with a mechanical two-sided cyclic die rotation system by an angle of up to  $\pm 12^\circ$ , at a frequency of up to 8 Hz. The maximum achievable extrusion rate (punch movement) equaled 2.0 mm/s. The press container's inner diameter equaled 40 mm and could be resistively heated to the initial temperature of 400 °C. In our own previous studies the used extrusion ratio  $\lambda$  were between 11.1 (usually 100) [1] and 10 000 [2].

The experiments conducted for this paper included both direct (Fig. 1a) and lateral (Fig. 1b) extrusion of materials, mainly carried out at room temperature (cold extrusion) – [4], and their in-depth analysis resulted in establishing effective parameters of the process with particular consideration of the extrudate properties (quality, mechanical parameters). The

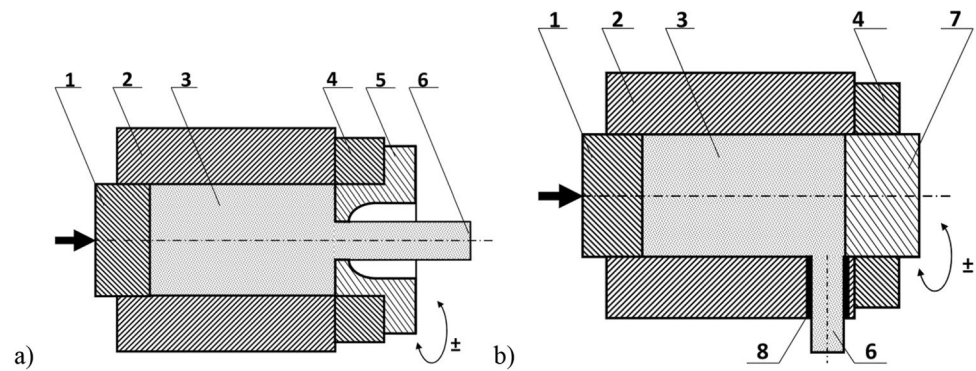
**Table 1** Chemical composition (wt.%) of the researched non-ferrous metallic alloys

Alloy	Al	Si	Fe	Cu	Mn	Mg	Cr	Zn	Ni	Ti	Li
2014	Balance	0.5–1.2	0.7	3.9–5	0.4–1.2	0.2–0.8	0.1	0.25		0.15	
7075	Balance	0.18	0.37	1.71	0.25	2.34	0.19	5.45	0.002	0.02	
Mg4Li						Balance					4
AZ91	8.7	Max. 0.01	Max. 0.012	Max. 0.01	0.17	Balance		0.76	0.001		
Cu6.5P	Max. 0.01	6.5P		Balance				Max. 0.05			
AK11	Balance	10.58	0.38	0.16	0.51	0.28	0.03	0.1	0.12	0.06	-

**Table 2** Chemical composition (wt.%) of Ti of the Grade 2 type

Material	Ti	N	C	Fe	H	Mg	O	Other
Ti Grade 2	Balance	0.01	0.02	0.1	0.002	0.2–0.8	0.13	<0.4

**Fig. 1** Scheme of direct (a) and lateral (b) extrusion by the KOBO method: 1 – punch, 2 – container (recipient), 3 – extruded material, 4 – lock, 5 – reversibly rotating die, 6 – product, 7 – reversibly rotating mandrel, 8 – die located on container's side surface



usual reverse die rotation angle and frequency values were  $\pm 8^\circ$  and 5 Hz respectively. Another variant of the experiment involved a systematical reduction of the frequency value during the process from 8 to 3 Hz in order to maintain constant extrusion force [1, 5]. According to formula (1) it should result in a constant viscosity coefficient  $\eta$ , and therefore the same deformation mechanism throughout the whole process. In this case, regardless of the material's self-induced heating (e.g. for aluminum from room temperature to over  $300^\circ\text{C}$  – [6]), the structure and mechanical properties of the obtained product remain identical along its whole length.

### 3 Results

#### 3.1 Mg-Li alloy

Products made of the MgLi alloy are usually manufactured by die-casting, due to their low formability. It is particularly true in the case of alloys with a HCP (Hexagonal Close Packed) structure, containing up to 5.7 wt.% Li (Mg solid solution). That is why alloys where the addition of Li varies between 5.7 and 10.3 wt.% with duplex phase structure, containing both  $\alpha$  – Mg phase and  $\beta$  – Li phase (Li solid solution, Body-Centered Cubic structure), are of more importance. Because phase  $\beta$  has excellent formability [7], alloys with the structure of  $\alpha + \beta$  can be successfully subjected to plastic deformation. Unfortunately, despite high specific yield strength ( $\sim 160 \text{ kN}\cdot\text{m}\cdot\text{kg}^{-1}$ ) in practice they display low mechanical strength, and raising their utility properties involves applying additional procedures, such as cold working [8], addition [9] of alloying elements (Zn, Al, Y ...) or precipitation hardening [10].

Even though in comparison with typical Mg alloys, the mechanical strength of Mg–Li alloys is much lower even after SPD (Severe Plastic Deformation) processing [11], it is assumed that light-weight magnesium alloys can be successfully used in automotive [12], aerospace [13], as well as in electronic [14] and implants production [15]. Attempts at plastic deformation of hardly-deformable single-phase ( $\alpha$

– Mg) MgLi alloys, particularly via high-temperature extrusion, are also carried out [16].

For this paper, the possibilities to apply the KOBO method for low-temperature extrusion of a magnesium alloy with 4 wt.% Li were explored. To this end, non-homogenized ingot  $\varnothing 40 \text{ mm}$  from Mg–4wt.%Li alloy was subjected to lateral KOBO extrusion at room temperature, as a result of which a wire with a diameter of 0.4 mm ( $\lambda = 10000$ ) was obtained. The extrusion rate was 0.5 mm/s. The initial die rotation frequency of 8 Hz was reduced during the process in order to maintain a constant extrusion force of 700 kN. Immediately after leaving the die the wire was cooled with a stream of air at room temperature and the pressure of 5 atm.

The lateral extrusion was chosen due to the construction of the press, because only this way allows to lead the wire immediately after it left the die. During direct extrusion the product in the shape of a thin wire cannot freely pass the distance of around 400 mm from the die to the exit of the press and usually gets tangled up, therefore blocking the press exit channel and terminating the procedure. It is important to point out that regardless of the direction of the KOBO extrusion the material follows identical mechanism (stratified flow) as for liquids according to the Pascal law. It was experimentally proved [4] that the actual parameters of direct and lateral KOBO extrusion require the same process parameters and lead to the same mechanical properties of the extrudates.

With such conditions of the process set, the aim was to gather precise information on the possibilities of intensifying the currently used industrial multi-staged process of manufacturing surgical sutures. Obviously, at the very high deformation rate the heat generated during the KOBO procedure leads to a significant rise in the alloy's temperature. Despite cooling both the alloy and the tools, the temperature of the extruded wire in place of leaving the die was around  $200^\circ\text{C}$ , which undoubtedly influenced the relatively low strength properties.

The image of the wire as well as its structure and strength properties are presented in Fig. 2. The quality of the wire (its surface state) was assessed as very good. The observed

fibrousness of structure is typical for low-temperature extruded metals and alloys.

Electron microscopy observations (Fig. 3) indicate the presence of low density dislocations forming homogeneously distributed very small cells, which can be linked to the fact that a dynamic recovery occurs during the process. Mechanical properties of the wire revealed by tensile test are very attractive:  $YS = 198 \text{ MPa}$ ,  $UTS = 281 \text{ MPa}$ ,  $A = 10\%$ . The tensile curve has a distinct Lüder's type plasticity boundary and a developing Portevin-Le Chatelier effect. In comparison, Mg–3wt.%Li alloy [16] prepared by casting reached  $YS = 55 \text{ MPa}$ ,  $UTS = 95 \text{ MPa}$  and  $A = 6\%$  during tensile test, while during compressive test:  $CYS = 51 \text{ MPa}$ ,  $UCS = 276 \text{ MPa}$  and  $A = 29.3\%$ . The alloy additionally subjected to extrusion at high ( $300 \text{ }^\circ\text{C}$ ) temperature with

the extrusion ratio  $\lambda$  of 79, obtained the following parameters:  $YS = 88 \text{ MPa}$ ,  $UTS = 175 \text{ MPa}$ ,  $A = 12.3\%$  and  $CYS = 75 \text{ MPa}$ ,  $YCS = 330 \text{ MPa}$  and  $A = 15\%$ .

In paper [17], comparative strength parameters for dual-phase structured Mg-Li alloys (6.24÷9.98 wt.% Li) prepared by melting, casting into a steel mold and subjected to compression test were given. A mixture of  $\alpha$  and  $\beta$  phases made it possible to obtain  $YS$  values of between 91.8÷85.1 MPa, while the stress corresponding to compressive strain equal to 35% was 300÷250 MPa.

### 3.2 Cu6.5P alloy

Dual phase Cu-P alloys, particularly Cu–6.5wt.%P, are known as extremely good solders that do not require flux

**Fig. 2** Ingot of Mg4Li magnesium alloy and wires produced out of it by low-temperature KOBO extrusion (a); microstructure (b) and mechanical properties (c) of the wire

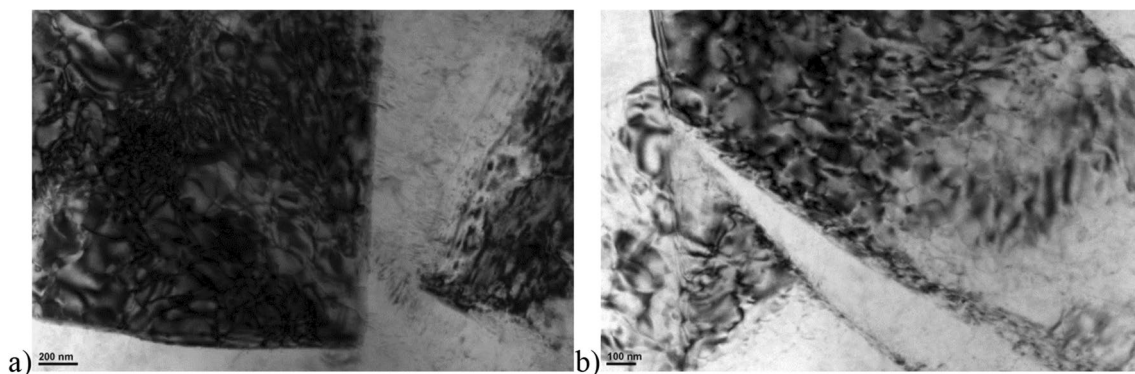
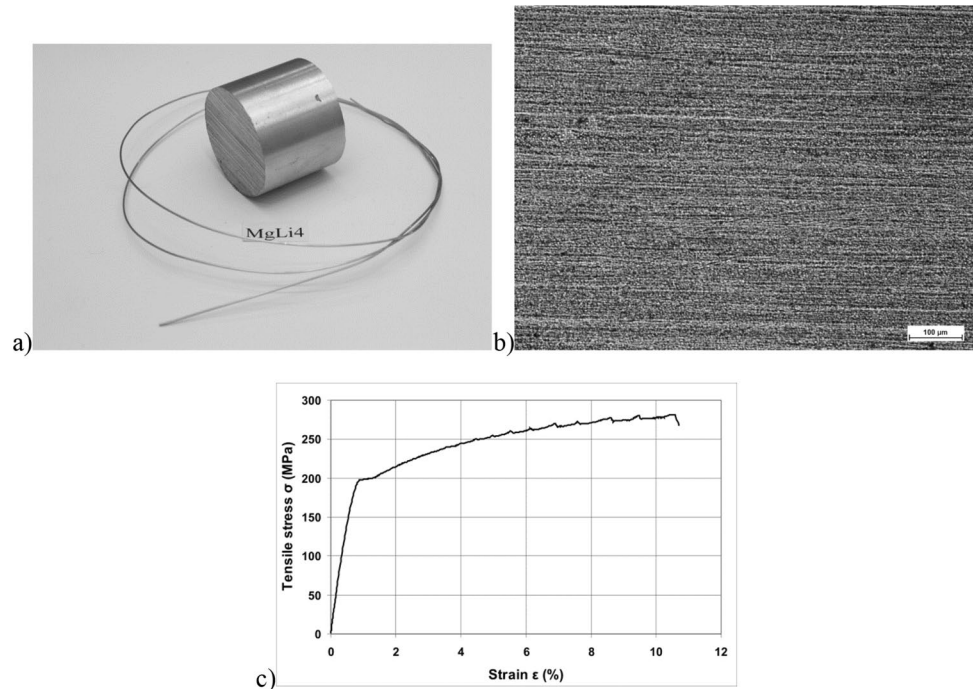


**Fig. 3** Microstructure of Mg4Li wire extruded by KOBO method with the ratio  $\lambda = 10000$ ; (a, b) different magnifications

application [18]. Unfortunately, their plastic deformation from ingots into final extrudates with a required geometry (such as wires or tapes) is very difficult due to the material's low plasticity. That is why they are mostly extruded at high temperatures [19] and subsequently subjected to plastic forming and heat treatment [20]. Low formability of the Cu–6.5wt.%P ingots is a consequence of their structural composition, which is a mixture of  $\alpha$  (P solution in Cu) and  $\text{Cu}_3\text{P}$  (eutectics) as well as large dendrites of the  $\alpha$  phase. Phase  $\alpha$  is plastic, but in the company of hardly-deformable  $\text{Cu}_3\text{P}$  phase, the Cu–6.5wt.% P alloy has a significantly lower susceptibility to plastic deformation, particularly at low (room) temperature.

For the purposes of this paper, an ingot from the Cu6.5P alloy was prepared via semi-continuous casting. The extrusion ratio  $\lambda$  of the direct KOBO extrusion was 100 (wire  $\text{Ø}4$  mm), extrusion rate equaled 0.5 mm/s, and the double-sided

die rotation angle  $\gamma = \pm 8^\circ$ . Other parameters of the process are presented in the scheme in Fig. 4.

The registered values included extrusion force, torque and displacement. The extrudate was subjected to structural observations and tensile testing at the rate of  $8 \times 10^{-3} \text{ s}^{-1}$ , however the results were linked to the parts where the samples were taken from (beginning, middle and end of the wire).

Two examples of mechanical characteristics of KOBO extrusion are given in Fig. 5. The first one corresponds with constant die rotation frequency of 8 Hz (dropping extrusion force), while the other shows the parameters for the process with constant extrusion force value (systematically reduced frequency with the initial value of 8 Hz). Summarized data on the impact of temperature on the maximum extrusion force and corresponding torque are shown in Fig. 6. Both, the process temperature and twisting frequency, have practically no impact on the maximum extrusion force, as opposed to torque. In this case the most significant changes occur at the frequency of 5 Hz, when the torque value drops by around 30% due to the rise in temperature from room temperature to 400 °C.

Figure 6 also provides an important information confirming the data presented in [1] that the higher twisting frequency (of 8 Hz) does not require higher torque values than the lower twisting frequency (of 5 Hz). Additionally, taking the extrusion force into account it can be stated that the KOBO extrusion at the frequency of 8 Hz consumes less energy than the process at the frequency of 5 Hz, which indicates particularly favorable contribution of the so called „structural factor”.

Tensile curves of the wire produced according to different variants of the KOBO extrusion are similar (Fig. 7). However, samples taken from the beginning of the wires show low elongation ( $A \approx 4\%$ ), while in the samples taken from other sections its values reach around 30% and apart from the range of high rise in shear stress – visible in all of the

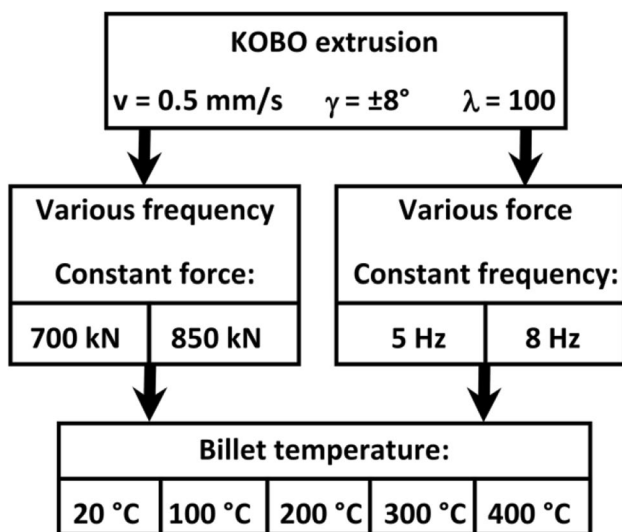


Fig. 4 Variants of extrusion by the KOBO method of Cu6.5P alloy

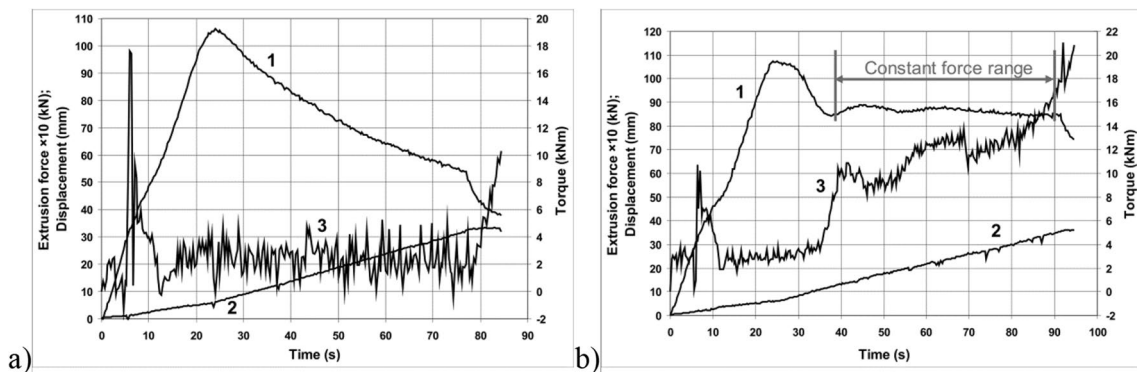
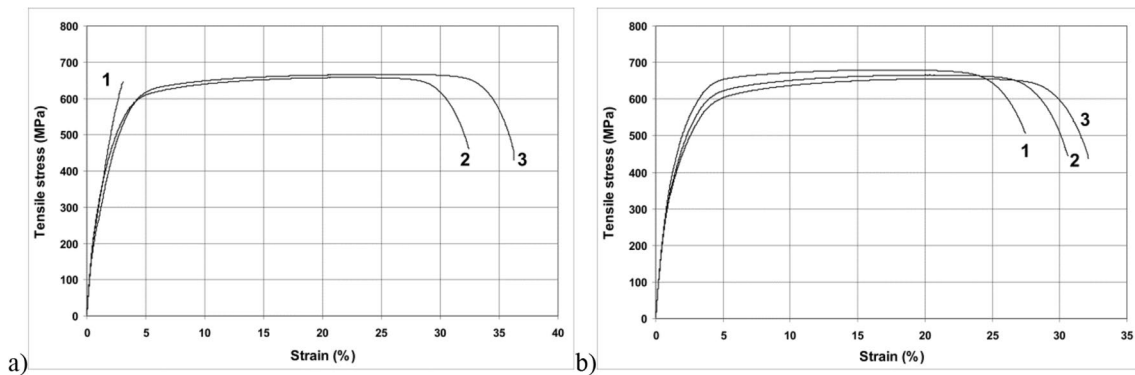
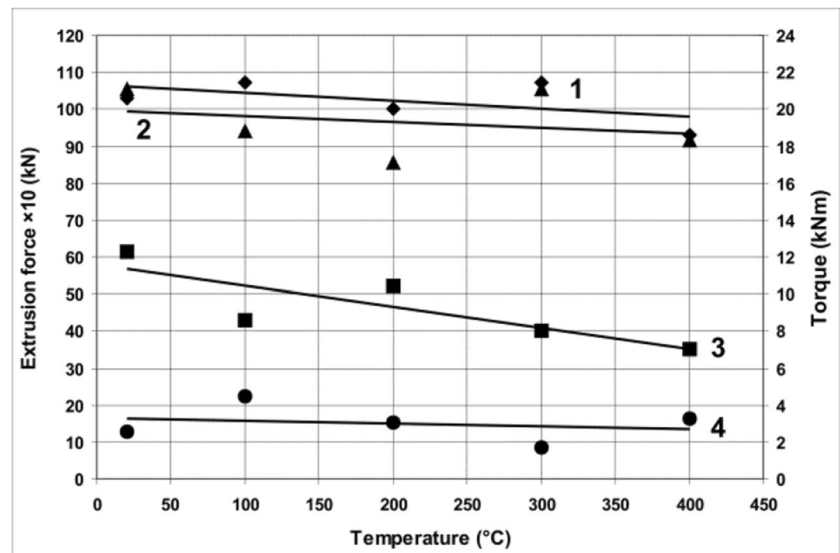


Fig. 5 Mechanical characteristics of KOBO extrusion of Cu6.5P alloy at room temperature: a) extrusion with constant frequency; b) extrusion with constant force. Note: 1 – extrusion force; 2 – displacement; 3 – torque

**Fig. 6** The impact of temperature and die oscillation frequency on the maximum extrusion force and torque in Cu6.5P alloy extruded by the KOBO method. Note: 1,2 – extrusion force; 3,4 – torque; data for die oscillation frequency of 5 Hz (1,3) and 8 Hz (2,4)



**Fig. 7** The impact of KOBO extrusion temperature at constant die oscillation frequency of 8Hz on the mechanical characteristics of the Cu6.5P alloy: a) 20 °C; b) 200 °C. Note: 1 – beginning, 2 – middle, 3 – end of the wire

samples – they have relatively wide „plateau” and at the end, the stress is gradually reducing, which is linked to the formation of neck and eventual destruction of the samples.

The results of the Cu6.5P compact tensile testing prove (Fig. 8) that regardless of the KOBO extrusion temperature, die rotation frequency and the place where the sample is taken from (with the exception of the beginnings of the wires), there are no major differences in the mechanical properties of the products. The mean values of yield stress, tensile strength and elongation, particularly for the twisting frequency of 5 Hz in the samples taken from the middle and end sections of the wire are 460 MPa, 670 MPa and 30% respectively, while for the frequency of 8 Hz they equal 450 MPa, 665 MPa and 32%. Significantly different mechanical properties at the beginnings of wires result from the need to initiate the phenomenon of plastic flow in the alloy in order to obtain a high enough concentration of point defects. In other words, the aforementioned phenomena can only occur

if the load in the press container undergoes cyclic change of deformation path, dislocation dipoles are formed and subsequently disintegrate into separate point defects.

The strength properties of the compact obtained at room temperature during the KOBO extrusion with constant extrusion force depend on the force's value, although in the conducted experiments they were each time higher than under the conditions of constant twisting frequency and have slightly lower elongation for the extrusion force of 850 kN or higher for the force of 700 kN, as shown in Fig. 9. Average parameters of the wires were as follows: YS  $\approx$  580 MPa, UTS  $\approx$  760 MPa, A  $\approx$  18% at the force of 850 kN and differ from the ones observed in the wires produced at the frequency of 8 Hz by 25; 14 and –22% respectively. On the other hand, at the extrusion force of 700 kN, the mechanical properties are as follows: YS  $\approx$  570 MPa, UTS  $\approx$  695 MPa, A  $\approx$  30%, and therefore higher than the values obtained by the wires extruded at the frequency of 8 Hz by 23; 4.2 and 30% respectively.

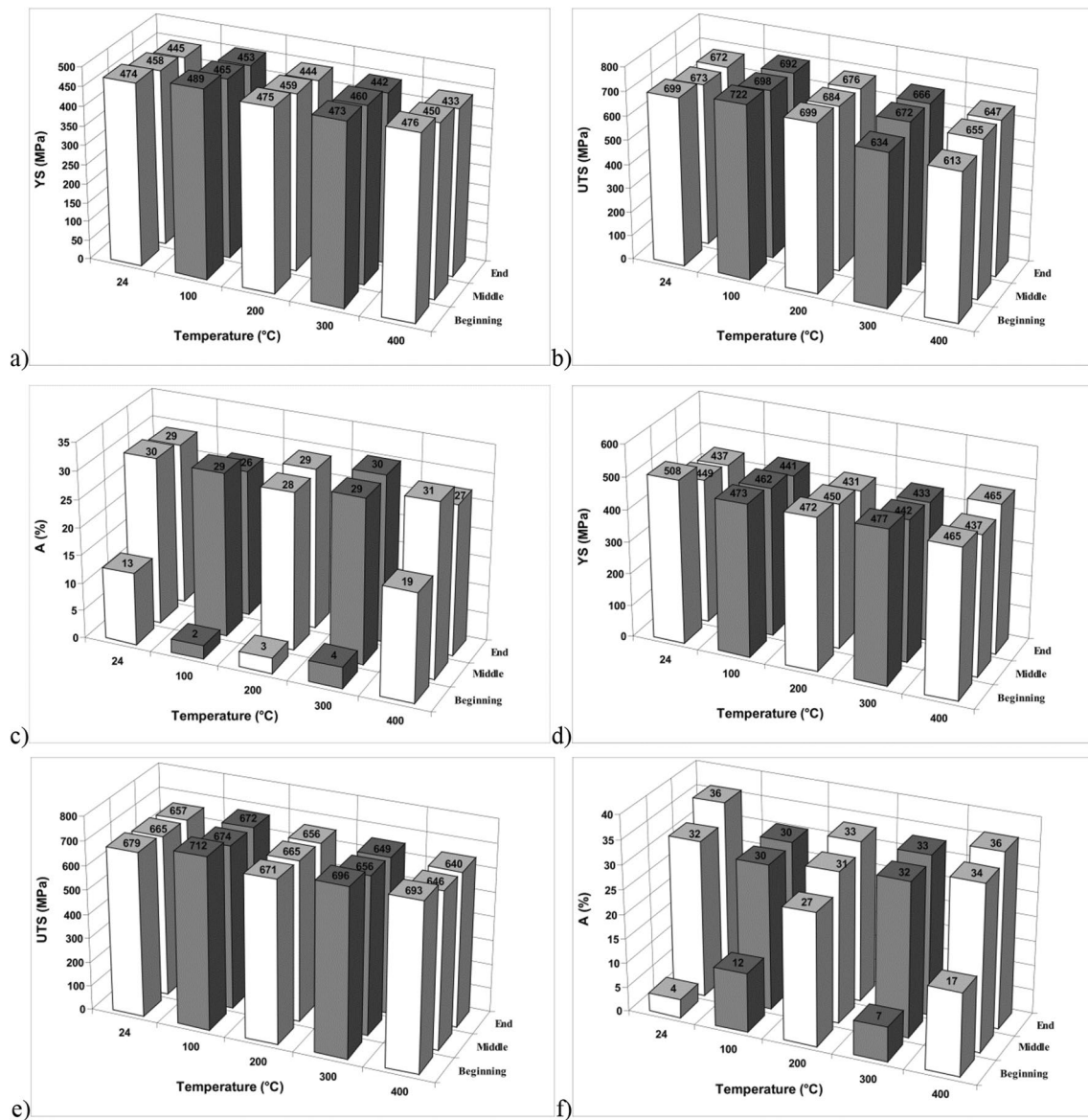


**Fig. 8** The impact of the load heating temperature and die oscillation frequency on the mechanical properties of wires (beginning, middle and end sections) made of Cu6.5P alloy extruded by the KOBO method; die rotating frequency 5 Hz (a-c), 8 Hz (d-f)

In Fig. 10, the structure of a Cu6,5wt.%P alloy ingot is shown, while Fig. 11 presents a typical structure of the wire extruded by the KOBO method. Regardless of the extrusion parameters, the extrudate ( $\varnothing 4$  mm wires) has a fragmented and highly homogeneous structure, without dendrites (Fig. 11). The observations of transverse micro sections of the wire extruded at room temperature with the frequency of 8 Hz (Fig. 11a,b) indicate minor differences in grain sizes at the beginning and end of the wires, however smaller grains are always observed in the initial fragments of the extrudate. In the case of extrusion with constant force the differences are not noticeable (Fig. 12). In longitudinal sections (Fig. 11c,

d and 12c,d) a typically fibrous structure linked to the direction of plastic flow of the extruded alloy is additionally visible.

### 3.3 AK11 aluminum alloy

Aluminum and silicon form a eutectic bond  $\alpha + \beta$ , although at room temperature the components practically do not dissolve in one another. Large  $\beta$ -phase dendrites have a negative impact [21] on both strength properties and plasticity of the Al-Si alloys (silumins), which depending on Si content can be highly creep resistant and have good load-carrying capacity [22].

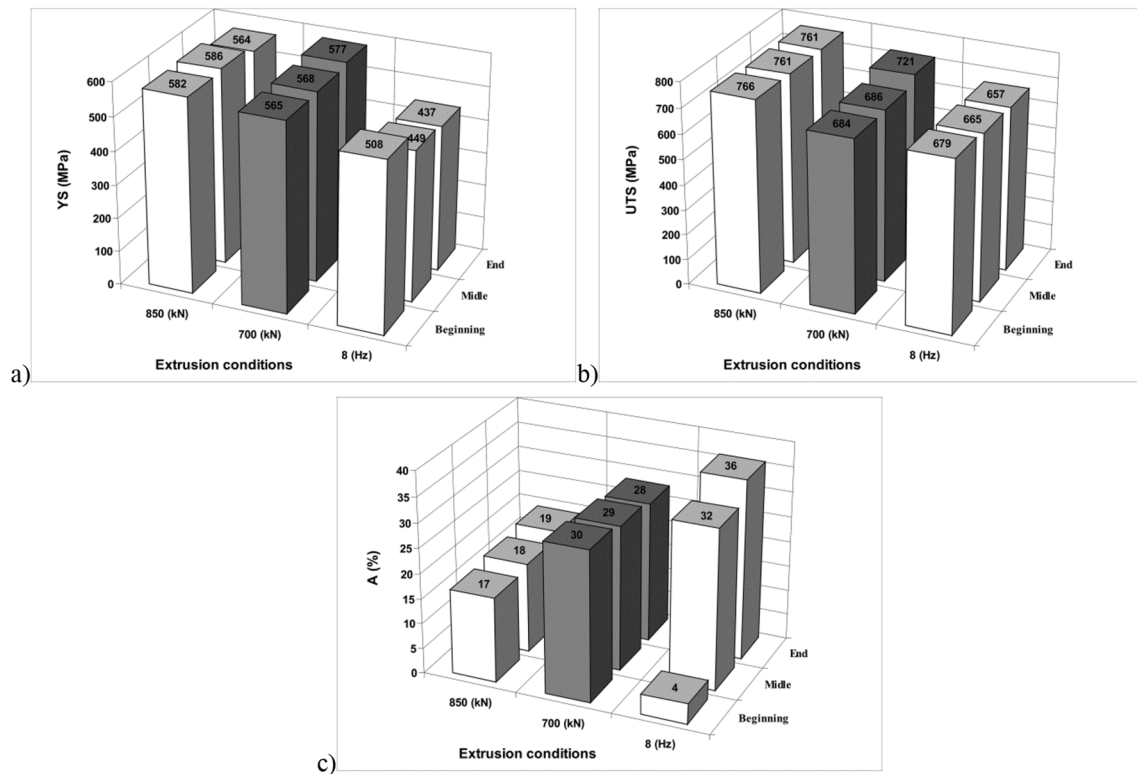


**Fig. 9** The impact of KOBO extrusion conditions at room temperature on the mechanical properties of wires made of Cu6.5P alloy (beginning, middle and end sections)

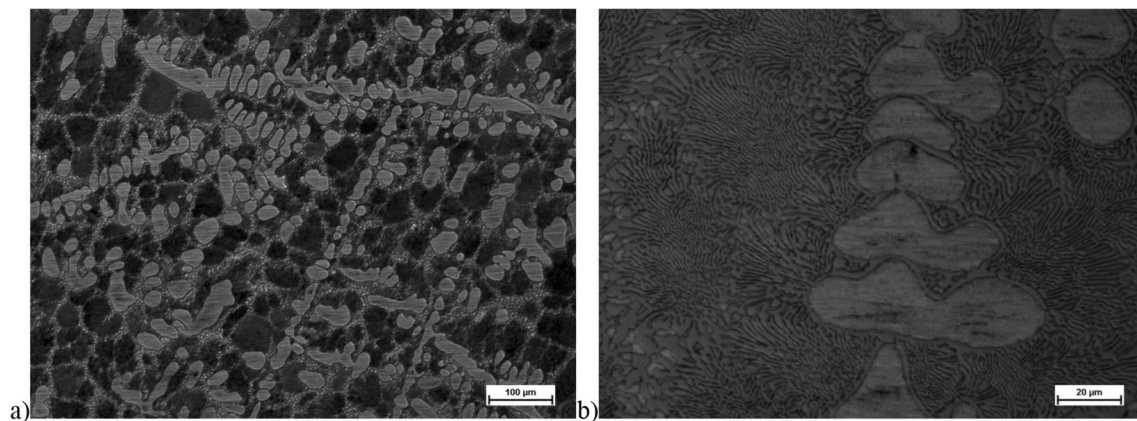


**Fig. 10** The structure of a semi-continuous casting of the Cu6.5P alloy; (a, b) various magnifications

It is commonly assumed that silumins can be plastically deformed up to just over 1 wt.% silicon content and those with high silicon content (10–23 wt.%) have good casting properties. However, the expectations regarding silumins do not follow their usual classification, for instance the Al–11 wt.% Si alloy is an indispensable material for overlay welding (counteracting the effects of misruns), even though its manufacturing into an applicable form of wire with a diameter of 1.0 mm requires unusually complex procedures

from raising ingot formability to structure fragmentation through cooling or modification after casting.

The microstructures of as-cast Al–Si alloys are characterized by a nonuniformly distributed Si particles [23], coarse primary  $\alpha$  – Al dendrites and porosity [24]. Usually, they are subjected to heat-treatment, which consists of solutionizing at high temperature (e.g.: 495 °C) for a long time (8 hours), quenching in oil (at 35°) followed by tempering (at 175 °C for 6h) and finally cooling in ambient temperature



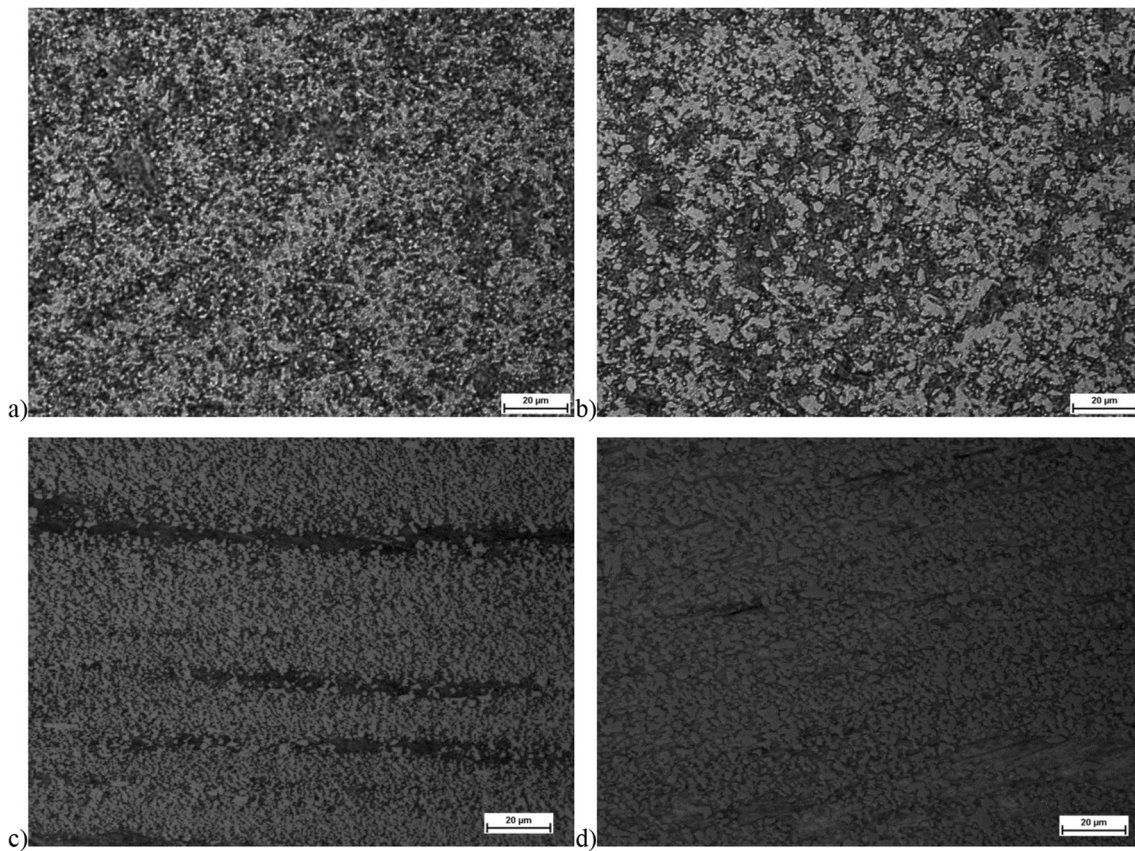


**Fig. 11** The structure of the Cu6.5P alloy extruded by the KOBO method at die oscillation frequency of 8 Hz and at room temperature: (a, b) cross-section; (c, d) longitudinal section; beginning (a, c) and end (b, d) of the wire

[25]. Examples of mechanical properties of an aluminum alloy containing 7.5wt.% Si (as well as 0.4Fe and 0.3Mg) in an as-cast state are as follows: YS = 113 MPa, UTS = 154 MPa, A = 2.7%, while after heat treatment YS = 196 MPa, UTS = 230 MPa, A = 3.3%.

The Al–11wt.% Si alloy in the form of a non-homogenized and unmodified ingot with the dimensions of  $\varnothing 40 \times 47$  mm was side-extruded at room temperature by the KOBO method into a wire with a diameter of 0.8mm ( $\lambda = 2500$ ). The extrusion rate was 0.2 mm/s and the initial die oscillation frequency equaled 5 Hz. The extrusion force was maintained at the level of 1000 kN. The compact was cooled at the press exit with a stream of air at room temperature. Figure 13 presents the structure of an ingot prepared for extrusion, the image of the  $\varnothing 0.8$ mm wire produced via the KOBO method, while Fig. 14 shows its fragmented structure. The tensile curve for the wire with characteristic Portevin–Le Chatelier strain instability is given in Fig. 15. The properties equaled YS = 162 MPa, UTS = 261 MPa and A = 7.5%. It is commonly assumed that the mechanical properties of the Al–Si alloys are dependent on the size, shape and distribution of eutectics and  $\alpha + \beta$  particles. Small, spherical and uniformly

distributed  $\alpha - \text{Si}$  particles increase the strength parameters of alloys. In comparison, the mechanical properties of the Al – 11.6wt.% Si ingot [26] are as follows: YS = 80 MPa, UTS = 185.4 MPa, A = 5.8%.

### 3.4 Recycling by the KOBO method

The most commonly applied metallurgic recycling method of metallic wastes (above all machining chips) is more often than not considered to be ineffective and unacceptable due to huge material losses (mainly its „burnout”), negative impact on natural environment, energy consumption [27] and high workload [28].

The main aim of KOBO extrusion of fragmented metallic fractions (wastes, chips) is to fully consolidate them into a solid product with a set geometry without the occurrence of liquid phase. Reaching satisfactory density and expected mechanical properties not differing from those obtained from a solid material/load via the KOBO method requires intimate adherence of neighboring and chemically active surfaces of various load fragments, which depends on the value of compressive strength (hydrostatic stress) and susceptibility to plastic deformation.

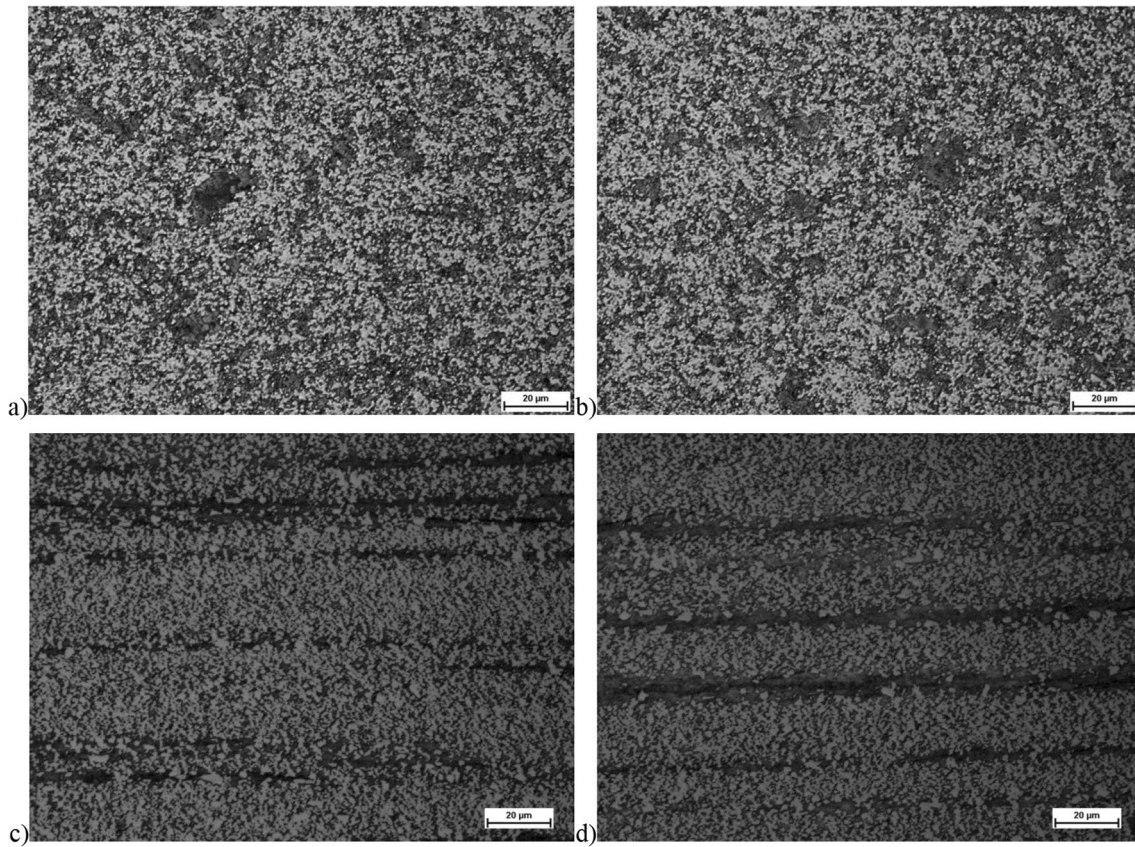


**Fig. 12** The structure of the Cu<sub>6.5</sub>P alloy extruded by the KOBO method at constant extrusion force of 850 kN and at room temperature: (a, b) cross-section; (c, d) longitudinal section; beginning (a, c) and end (b, d) of the wire

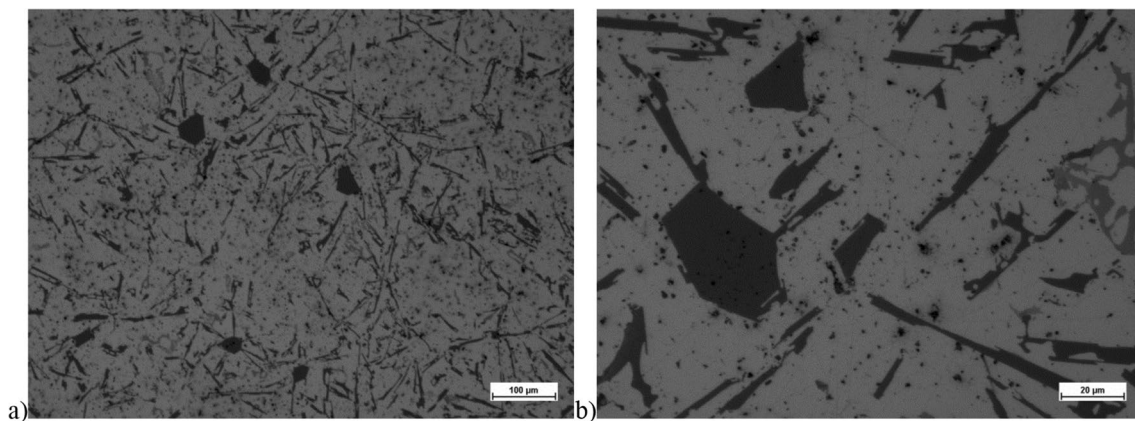


**Fig. 13** The structure of as-cast AK11 alloy; (a, b) different magnifications

Conventional high-temperature extrusion of fragmented fractions [29] usually does not guarantee satisfactory consolidation due to excess oxidation of the load and highly limited extrusion ratio  $\lambda$ , resulting from insufficient press force of the equipment (presses) usually used for that purpose [30]. On the contrary, low-temperature KOBO extrusion reveals „fresh” surfaces of load fragments (devoid of

oxides and other pollutants, e.g., remnants of emulsions from machining), which get closer to one another even under low stress, leading to the formation of atomic bonds between them. Localization of deformation also affects diffusion processes leading to their intensification, as the point defects in shear bands are the carriers of these phenomena and therefore become an additional consolidation factor.

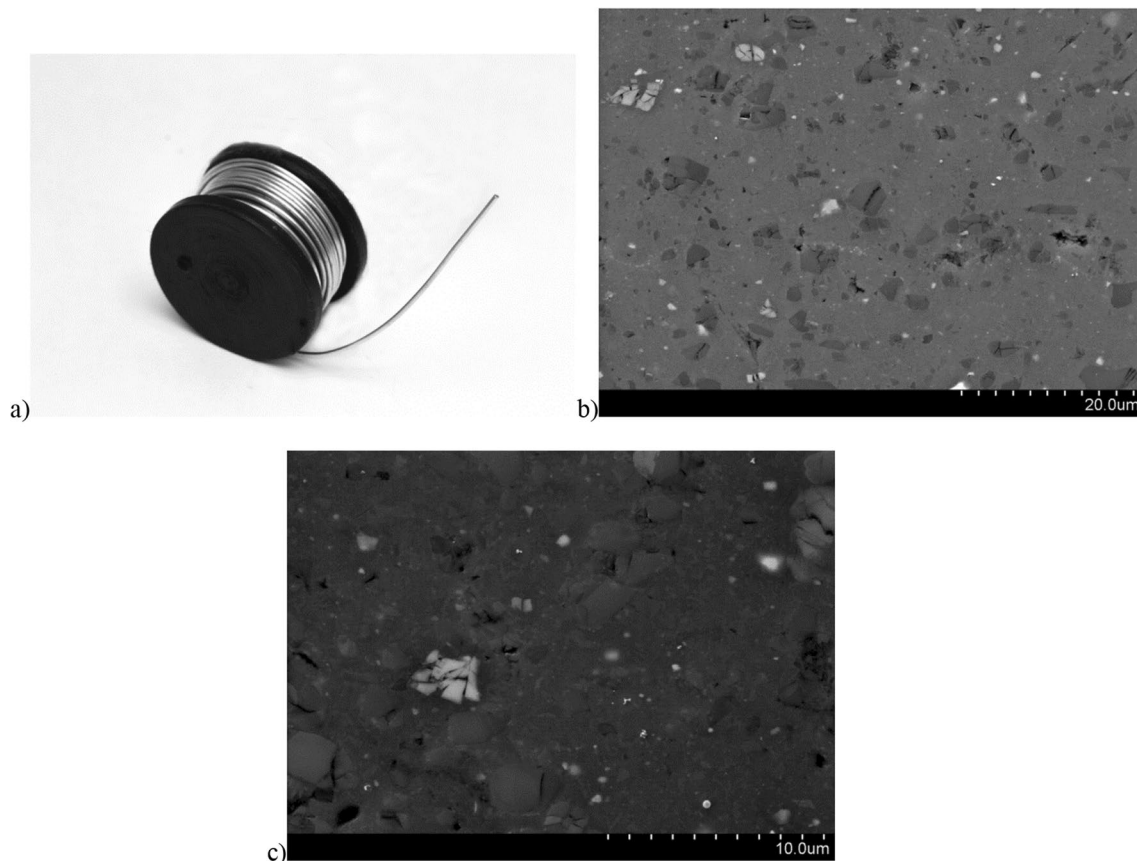


**Fig. 14** The image of wire (a) from the AK11 alloy extruded by the KOBO method at extrusion ratio  $\lambda = 2500$  ( $\text{Ø}0.8$  mm) and its fragmented microstructure (b, c)

### 3.4.1 Chips of aluminum alloys

Industrial chips of 2014 and 7075 alloys (Fig. 16a, b) were subjected to low-temperature (room temperature) extrusion by the KOBO method without any chemical or mechanical

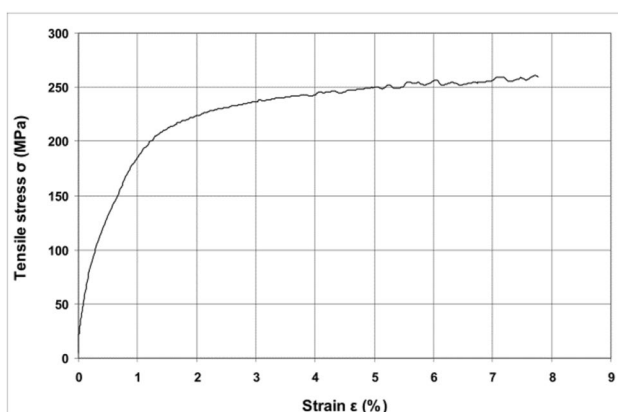


**Fig. 15** Mechanical characteristics of the 0.8mm wire made of AK11 alloy lateral extruded by the KOBO method

cleaning from the remnants of machining (turning) emulsions. The chips were earlier stored at room temperature in a place of low-humidity for a couple of days, where they were dried and subsequently densified under the pressure of 300 kN into briquettes (loads) with a diameter of  $\text{Ø}39.5$  mm and length of 50 mm (Fig. 16c, d). The KOBO extrusion process was carried out without pre-heating the loads, i.e., on a „cold press” (at room temperature) at the rate of 0.2 mm/s. Initial die rotation frequency of 8 Hz was systematically reduced in order to maintain the set, constant extrusion force (700 and 850 kN). Dies of different shapes and sizes of working apertures were used in order to obtain a compact with functional properties. The extrusion ratio was not high – between 25 and 40. Upon exit from the die, the compact was immediately cooled with cold water.

Examples of the KOBO process force characteristics are presented in Fig. 17, while Fig. 18 shows the image of the obtained compact.

Mechanical properties of the compact's circular section were established via tensile testing conducted at room temperature and the rate of  $8 \times 10^{-3} \text{ s}^{-1}$  (Fig. 19 and Table 3).

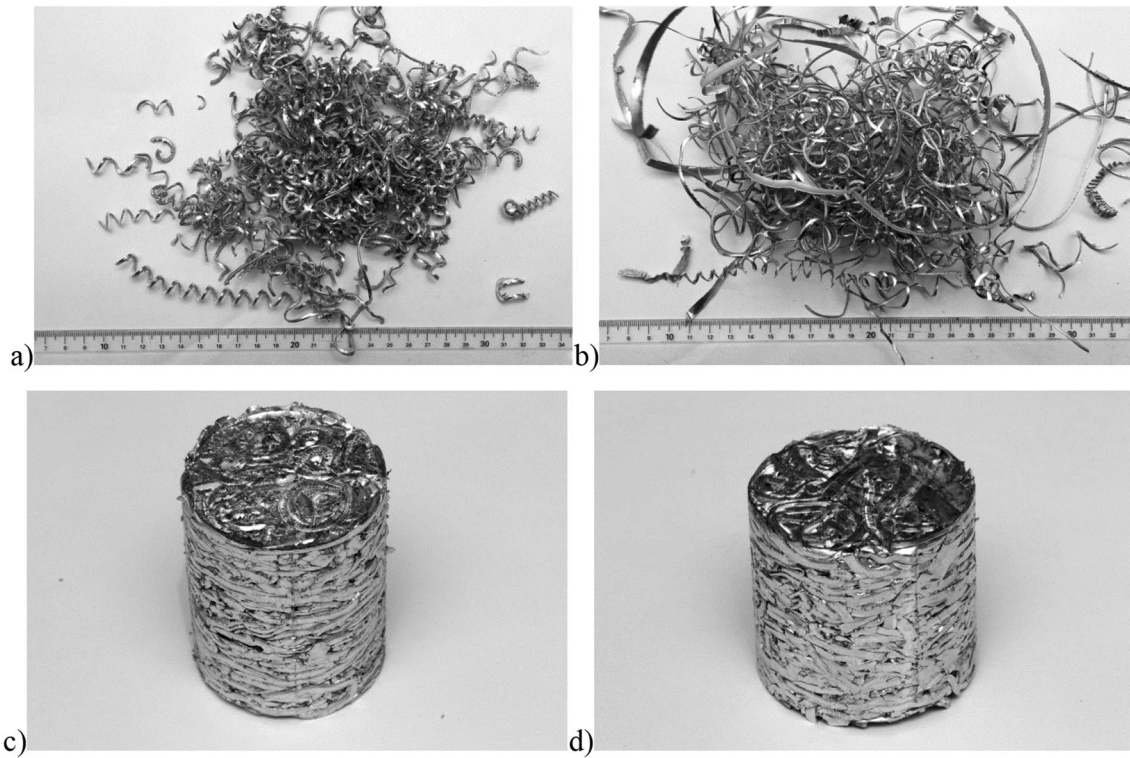


**Fig. 16** Examples of aluminum 2014 (a) and 7075 (b) chips and their compacted form (c, d) respectively

Tensile curves reveal a Portevin-Le Chatelier phenomenon commonly observed in alloys and the compact's mechanical properties are better than those recorded for products manufactured metallurgically after oversaturation. As proved in earlier papers (concerning the KOBO method), the mechanical properties of the compact - apart from the type of alloy - strongly depend on the extrusion ratio  $\lambda$ , extrusion rate and temperature, and most of all on the angle and frequency of die oscillation, in other words on the set parameters of the KOBO process. The higher the

processing degree  $\lambda$ , the more favorable the effect of consolidation. However, even under far from optimal experimental conditions ( $\lambda \geq 40$ ) no structural discontinuities in the compact were observed. Figure 20 presents typical structures of the wire obtained via consolidation of industrial chips from 2014 and 7075 alloys without the liquid phase. The process normally results in „irregularities” observed in cross-sections (flow lines are curved in opposite directions to one another – Fig. 20c) which result from double-sided twisting of the alloy during KOBO extrusion.

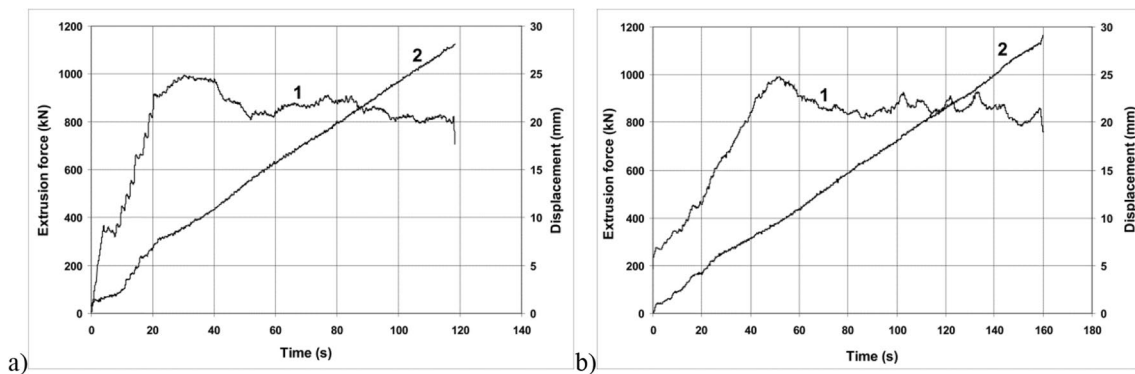


**Fig. 17** Curves of plastic consolidation of AA2014 industrial chips via KOBO extrusion: a) angle profile, b) I-beam. Note: 1 – extrusion force; 2 – displacement

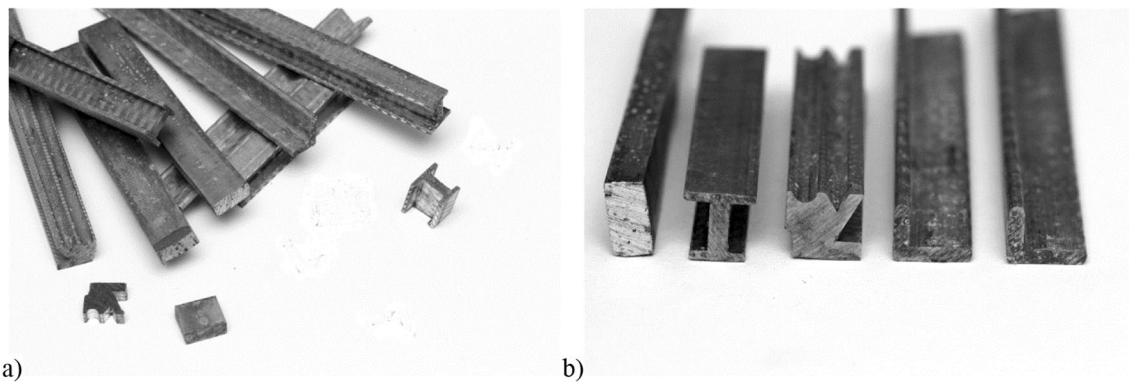


**Fig. 18** Images of profiles obtained by plastic consolidation of aluminum alloy industrial chips by the KOBO method: a) 2014; b) 7075

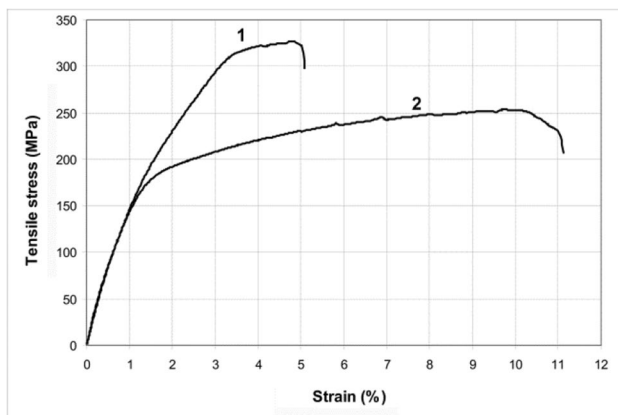


**Fig. 19** Tensile curves for  $\phi=6\text{mm}$  rods obtained by KOBO method consolidation of industrial chips from aluminum alloys 7075 (1) and 2014 (2)

**Table 3** Mechanical properties of aluminum alloys' compact obtained via plastic consolidation with the KOBO method

Material	YS (MPa)	UTS (MPa)	A (%)
7075	195	327	3.8
2014	179	254	10.1

### 3.4.2 AZ91 chips

The recycling of magnesium alloy machining chips while avoiding metallurgical processes is one of the current challenges in materials science. The complex nature of the process is exacerbated by the fact that the fragmented chips easily become oxidized and can catch fire, which significantly increases their processing costs. Therefore, establishing new recycling methods is of great importance.

Conventional high-temperature extrusion of machining chips does not lead to their satisfactory consolidation, due to the rather low processing ratio of the procedure [31]

and high near-surface oxidation of individual chips [32]. Attempts at solving the problem via the SPD methods [33], particularly ECAP (Equal Channel Angular Pressing) [34], and CEC (Cyclic Extrusion-Compression) [35] conducted to date, have proved to have low performance values and thus, their results do not encourage their implementation on an industrial scale. Taking this into account, the experimentally documented possibilities for consolidation of magnesium alloy machining chips via low-temperature KOBO extrusion opens both new research and practical opportunities.

Two types of chips of the AZ91 alloy were subjected to consolidation by low-temperature KOBO extrusion. One type was obtained via turning without the use of emulsions (under laboratory conditions) and the other with the use of emulsions (under industrial conditions). The chips were not cleaned thermally nor mechanically and were stored for 48h in advance in a place of room temperature and low humidity.

Modified load from initially briquetted chips and a small element blocking the die exit made from the same alloy in a solid state were used (Fig. 21) in order to prevent potential pushing of the unconsolidated or not fully consolidated chips at the very beginning of the process. Relevant shape of the blocking element guaranteed that the die rotation would be fully carried onto the briquette (which prevented „slipping” of the blockade upon touching the briquette).

In Fig. 22 mechanical characteristics of the compact obtained via KOBO extrusion from „clean” chips. Curve 1 corresponds with the beginning of the compact originating from the solid alloy (blocking element), while other curves correspond with the compact produced from chips consolidated during KOBO extrusion, including its end parts – curves 2.

Microstructures of the extrudate obtained from chips are shown in Fig. 23. The same set of results for industrial chips (i.e., polluted with emulsion) is presented in Figs. 24 and 25.

The obtained results were rated as satisfactory. The use of the element blocking the flow of compact made it

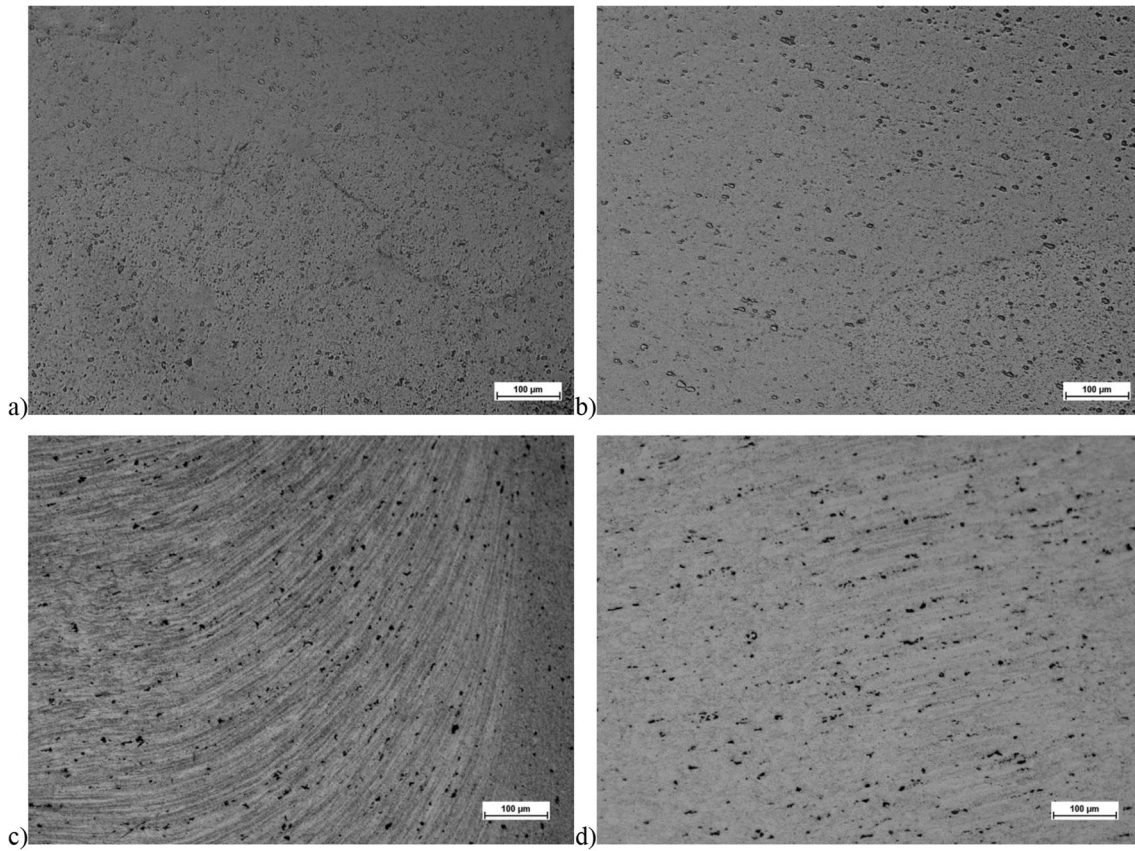


**Fig. 20** Structures of profiles extruded by the KOBO method from industrial chips of the 2014 alloy (a, b) and 7075 alloy (c, d); cross-section (a, c); longitudinal section (b, d)

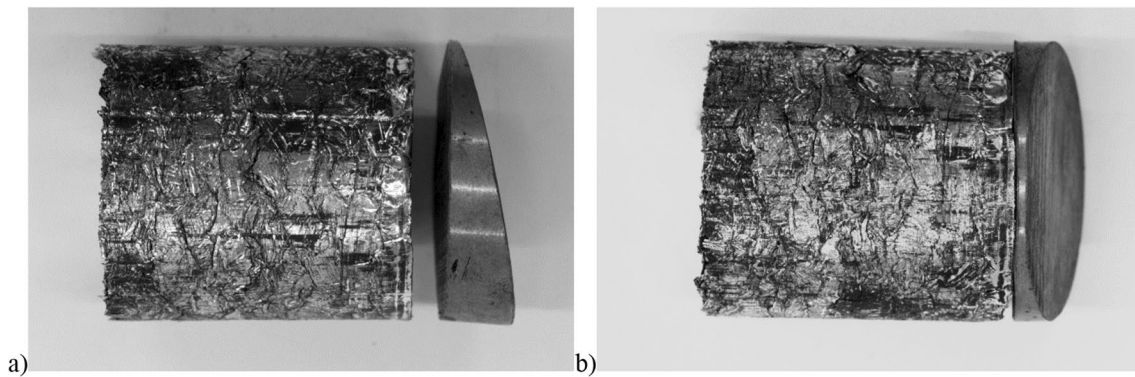


**Fig. 21** Image of the AZ91 magnesium alloy briquette in the form of compacted chips with the additional blocking element („blockade”); decomposition of load (a) and prepared for extrusion (b)

possible to maintain a relatively high and constant extrusion force throughout the KOBO procedure, which is extremely difficult in the case of extrusion of fragmented fractions controlled merely via reduction of die oscillation frequency. As a result  $\text{Ø}4$  mm rods of good quality were obtained at room temperature from AZ91 alloy chips the

density and mechanical properties of which correspond with those of their solid fraction.

### 3.4.3 Chips of titanium (Grade 2)

Titanium shows very high affinity to oxygen and nitrogen so melting its chips needs application of vacuum or an inert

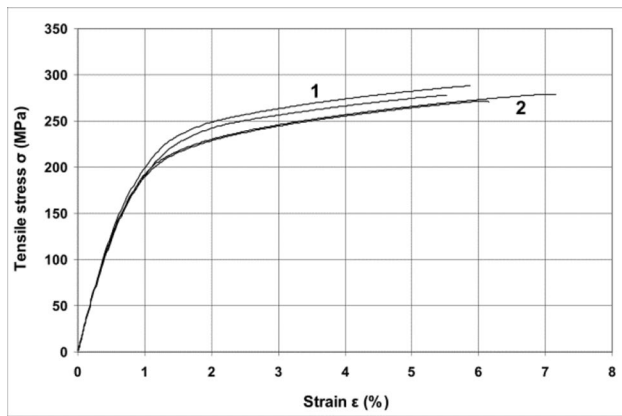


**Fig. 22** Tensile curves of wire made of cleaned AZ91 alloy chips consolidated by the KOBO method: 1 – beginning and 2 – ends of the wire

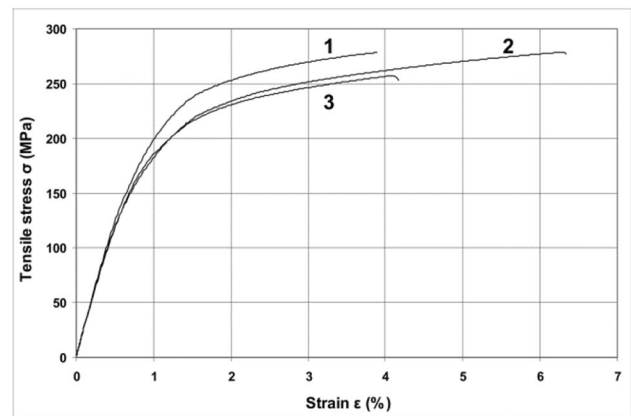


**Fig. 24** Tensile curves of wire made of emulsion-polluted AZ91 alloy chips consolidated by the KOBO method: 1 – beginning; 2 – middle and 3 – end of wire

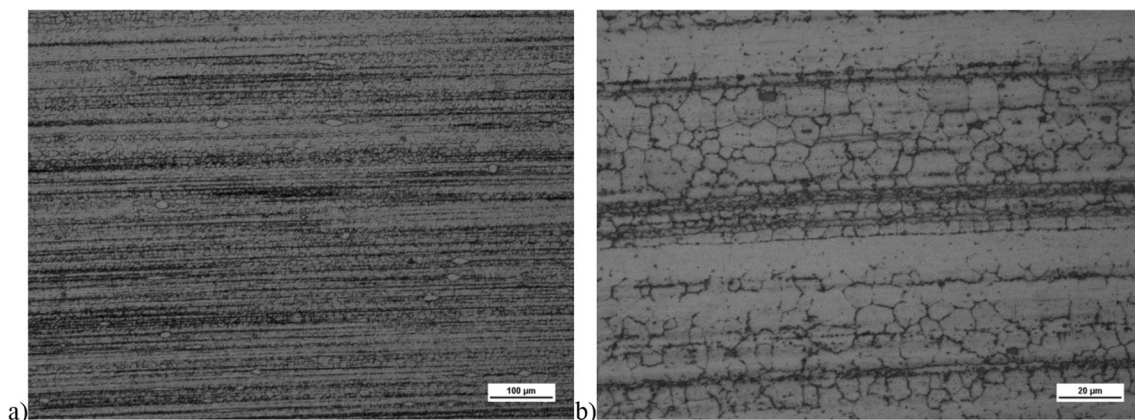
gas. Low-temperature KOBO extrusion makes its recycling significantly easier. In order to confirm the effectiveness of the process, studies on titanium (Grade 2) chips consolidation on the KOBO press at the temperature of 350 °C were conducted. At such temperature the chips do not yet recrystallize and the process of compact flow could be initiated. It was necessary due to high plastic flow resistance of Ti, as even the maximum press force (1100 kN) turned out too low to initiate the process at room temperature. On the other hand, due to prolonged passive oscillation the die wore quickly. It is important to point out that after initiating the process at 350 °C, at the rate of 0.1 mm/s, double-sided die rotation frequency of 5 Hz and extrusion ratio  $\lambda=25$ , it was constantly carried out with the maximum pressing force.

Figure 26 shows subsequent stages of Ti (Grade 2) chips consolidation via KOBO extrusion, the compact structure and its mechanical properties. Based on this data, it can be assumed that low-temperature KOBO extrusion of titanium chips can be successfully applied for recycling without the liquid phase.

Interesting data on Ti chips consolidation via the KOBO method can also be found in paper [36], which focuses on the assessment of compact density, structural observations and mechanical properties measurements depending on the place of sampling. It was established that the extrudate had a small number of voids [37, 38] and a homogeneous grained structure and that the mechanical properties of the extrudates/rods were close to that of titanium from which the chips were produced.

## 4 Summary

In the recently published paper [3] on the possibilities of controlling the structure and mechanical properties of metals through the application of particular plastic deformation scheme, the following important statement was made:



**Fig. 23** Microstructures of wire made of cleaned AZ91 alloy chips consolidated by the KOBO method; (a, b) different magnifications

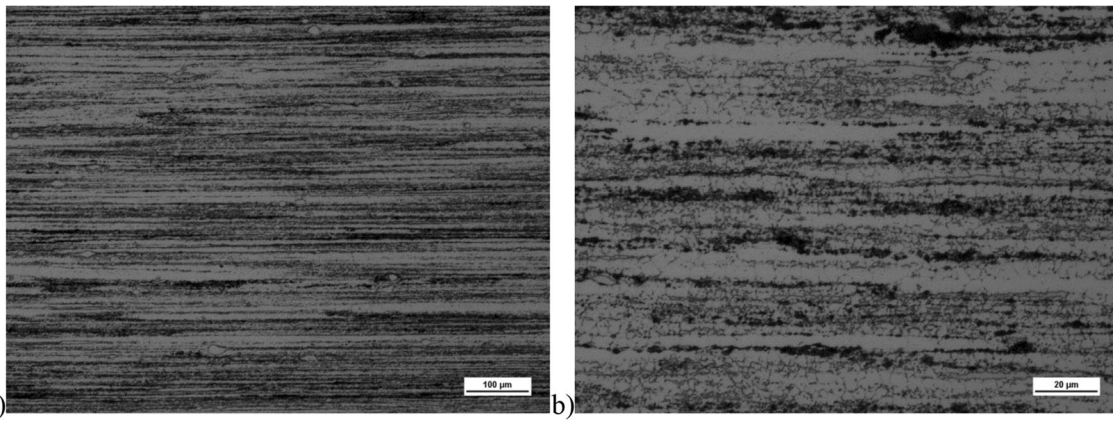


**Fig. 25** Microstructures of wire made of emulsion-polluted AZ91 alloy chips consolidated by the KOBO method; **(a, b)** different magnifications

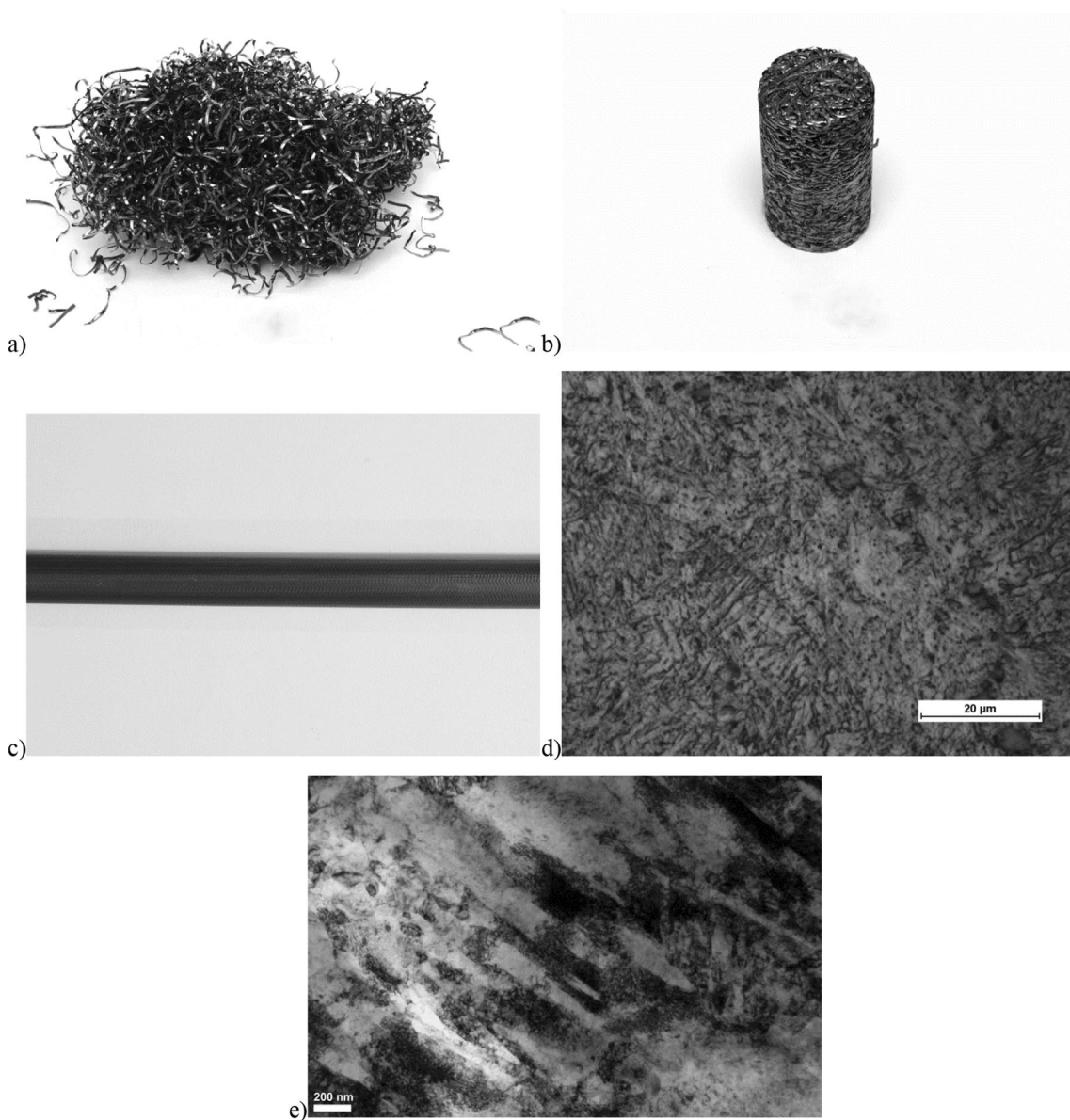


**Fig. 26** Subsequent stages of titanium Grade 2 chips consolidation via the KOBO method: **a)** chips; **b)** briquette; **c)** extrudate/rod; **d)** rod structure; **e)** rod microstructure (TEM)



*“Therefore, a question whether using quite complicated technological measures has already allowed to obtain the best possible properties of a metallic material, which has already been deformed or is undergoing a deformation process or, in other words, whether potential properties generated by plastic deformation processes in the structure of metallic materials have been used to their maximum, is worth asking”.*

Experimental results obtained for the purpose of this paper point to new areas of research and prove that it is worth exploring them in order to find innovative solutions based on the twenty year old concept of Structure Based Design of Metal Forming Operations (SBD-MFO) [39]. Particularly the KOBO method, developed as a result of this concept, is key to highly economical industrial production processes involving plastic deformation of hardy-deformable metallic materials not only in solid state but also in fragmented fractions (chips), as it significantly impacts their structural state both during and after the KOBO procedure. i.e., the structure of extrudates (post-deformation effect), guaranteeing their high functional properties.

**Author contribution** Włodzimierz Bochniak contributed to the conceptualization, methodology, investigation, writing – original draft; Paweł Ostachowski contributed to the conceptualization, methodology, investigation, writing – review and editing; Andrzej Korbel contributed to the conceptualization, methodology and investigation; Marek Łagoda contributed to the conceptualization, investigation and funding.

**Funding** The work was supported by the National Science Center of Poland under Project No UMO-2019/03/X/ST8/01924.

## Declarations

**Ethical statement** The research was done according to ethical standards. Author ensure that the work described has been carried out in accordance with Publishing Ethics

**Conflict of interest** The authors declare that they have no conflict of interest.

**Open Access** This article is licensed under a Creative Commons Attribution 4.0 International License, which permits use, sharing, adaptation, distribution and reproduction in any medium or format, as long as you give appropriate credit to the original author(s) and the source, provide a link to the Creative Commons licence, and indicate if changes were made. The images or other third party material in this article are included in the article’s Creative Commons licence, unless indicated otherwise in a credit line to the material. If material is not included in the article’s Creative Commons licence and your intended use is not permitted by statutory regulation or exceeds the permitted use, you will need to obtain permission directly from the copyright holder. To view a copy of this licence, visit <http://creativecommons.org/licenses/by/4.0/>.

## References

1. Korbel A, Bochniak W, Ostachowski P, Błaż L (2011) Viscoplastic flow of metal in dynamic conditions of complex strain scheme. *Metall Mater Trans A* 42A:2881–2897
2. Korbel A, Bochniak W (2017) Liquid like behavior of solid metals. *Manuf Lett* 11:5–7
3. Korbel A, Bochniak W (2017) Stratified plastic flow in metals. *Int J Mech Sci* 128–129:269–276
4. Bochniak W, Korbel A, Ostachowski P, Paliborek A (2013) Mechanical properties of aluminum extruded via the KOBO method with direct and lateral outflow. *Int J Mater Res* 104:974–979
5. Ostachowski P, Paliborek A, Bochniak W, Łagoda M (2022) Mechanical characteristics and structure of highly deformed zinc. *J Mater Eng Perform* 31:3638–3660
6. Korbel A, Bochniak W, Ostachowski P, Paliborek A, Łagoda M, Brzostowicz A (2016) A new constitutive approach to large strain plastic deformation. *Int J Mater Res* 107:44–51
7. Haferkamp H, Boehm R, Holzkamp U, Jaschik C, Kaese V, Niemeier M (2001) Alloy development, processing and applications in magnesium lithium alloys. *Mater Trans* 42:1160–1166
8. Takuda H, Kikuchi S, Tsukada T, Kubota K, Hattata N (2002) Tensile properties of a few Mg-Li-Zn alloy thin sheets. *J Mater Sci* 37:51–57
9. Yamamoto A, Ashida T, Kouta Y, Kim KB, Fukumoto S, Tsubakino H (2003) Precipitation in Mg-(4–13)%Li-(4–5)%Zn ternary alloys. *Mater Trans* 44:619–624
10. Chiu CH, Wu HY, Wang JY, Lee S (2008) Microstructure and mechanical behavior of LZ91 Mg alloy processed by rolling and heat treatments. *J Alloys Compd* 460:246–252
11. Xu DK, Zu TT, Yin M, Xu YB, Han EH (2014) Mechanical properties of the icosahedral phase reinforced duplex Mg–Li alloy both at room and elevated temperatures. *J Alloys Compd* 582:161–166
12. Kumar DS, Sasanka CT, Ravindra K, Suman KNS (2015) Magnesium and its alloys in automotive applications – a review. *Am J Mater Sci Technol* 4:12–30
13. Cain TW, Labukas JP (2020) The development of  $\beta$  phase Mg–Li alloys for ultralight corrosion resistant applications. *Mater Degradation* 4:1–10
14. Lv Y, Liu M, Xu Y, Cao D, Feng J (2013) The electrochemical behaviors of Mg–8Li–3Al–0.5Zn and Mg–8Li–3Al–1.0Zn in sodium chloride solution. *J Power Sources* 239:265–268
15. Chen XB, Li C, Xu D (2018) Biodegradation of Mg–14Li alloy in simulated body fluid: A proof-of-concept study. *Bioactive Mater* 3:110–117
16. Dong H, Pan F, Jiang B, Li R, Huang X (2015) Mechanical properties and deformation behaviors of hexagonal Mg–Li alloys. *Mater Des* 65:42–49
17. Kúdela S Jr, Švec P, Bajana O, Orovčík L, Ranachowski P, Ranachowski Z (2016) Strengthening in dual-phase structured Mg-Li-Zn alloys. *Kov Mater Met Mater* 54:483–489
18. Tavalzhanskii SA, Bazhenov VE, Pashkov IN (2016) Composition, properties, application, and manufacturing features of binary copper–phosphorus solders. *Metallurgija* 60:750–757
19. Sheppard T, Yiu HL (1984) Microstructure and properties of some extruded copper–phosphorus alloys. *Met Sci* 18:439–448
20. Yiu HL, Sheppard T (1985) Deformation of Cu–P alloys at high temperatures. *Mater Sci Technol* 1:209–219
21. Shivaprasad CG, Aithal K, Narendranath S, Desai V, Mukunda PG (2015) Effect of combined grain refinement and modification on

- microstructure and mechanical properties of hypoeutectic, eutectic and hypereutectic Al-Si alloys. *Int J Microstruct Mater Prop* 10:274–284
22. Ye H (2003) An overview of the development of Al-Si-Alloy based material for engine applications. *J Mater Eng Perform* 12:288–297
  23. Zhang B, Poirier DR, Chen W (1999) Microstructural effects on high-cycle fatigue-crack initiation in A356.2 casting alloy. *Metall Mater Trans A* 30A:2659–2666
  24. Seniw ME, Conley JG, Fine ME (2000) The effect of microscopic inclusion locations and silicon segregation on fatigue lifetimes of aluminum alloy A356 castings. *Mater Sci Eng A* 285:43–48
  25. Singh RK, Telang A, Das S (2016) Microstructure and mechanical properties of Al-Si alloy in as-cast and heat treated condition. *Am J Eng Res* 5:133–137
  26. Torabian H, Pathak JP, Tiwari SN (1994) Wear characteristics of Al-Si alloys. *Wear* 172:49–58
  27. Gronostajski J, Marciniak H, Matuszek A (2000) New methods of aluminium and aluminium-alloy chips recycling. *J Mater Process Technol* 106:34–39
  28. Tucholski G (2013) Chips versus briquettes: How the aluminium industry can effectively and efficiently recycle scrap. *Int Aluminium J* 89:87–88
  29. Ab Rahim SN, Lajis MA, Ariffin S (2015) A review on recycling aluminum chips by hot extrusion process. *Procedia CIRP* 26:761–766
  30. Wagiman A, Mustapa MS, Asmawi R, Shamsudin S, Lajis MA, Mutoh Y (2020) A review on direct hot extrusion technique in recycling of aluminium chips. *Int J Adv Manuf Technol* 106:641–653
  31. Wen L, Ji Z, Li X (2008) Effect of extrusion ratio on microstructure and mechanical properties of Mg–Nd–Zn–Zr alloys prepared by a solid recycling process. *Mater Charact* 59:1655–1660
  32. Mindivan H, Taskin N, Kayali ES (2014) Recycling of pure magnesium chips by cold press and hot extrusion processes. *Acta Phys Polon A* 125:429–431
  33. Valiev RZ, Islamgaliev RK, Alexandrov IV (2000) Bulk nanostructured materials from severe plastic deformation. *Prog Mater Sci* 45:103–189
  34. Ying T, Zheng MY, Hu XS, Wu K (2010) Recycling of AZ91 Mg alloy through consolidation of machined chips by extrusion and ECAP. *Trans Nonferrous Metals Soc China* 20:s604–s607
  35. Peng T, Wang QD, Lin JB (2009) Microstructure and mechanical properties of Mg–10Gd–2Y–0.5Zr alloy recycled by cyclic extrusion compression. *Mater Sci Eng A* 516:23–30
  36. Topolski K, Bochniak W, Łagoda M, Ostachowski P, Garbacz H (2017) Structure and properties of titanium produced by a new method of chip recycling. *J Mater Process Technol* 248:80–91
  37. Topolski K, Jaroszewicz J, Garbacz H (2021) Structural aspects and characterization of structure in the processing of titanium grade4 different chips. *Metals* 11:101 1–23.
  38. Topolski K, Ostachowski P (2021) Solid state processing of various titanium chips using unconventional plastic working method. *J Mater Res Technol* 13:808–822
  39. Korbel A, Bochniak W (1995) The structure based design of metal forming operations. *J Mater Process Technol* 53:229–237

**Publisher's note** Springer Nature remains neutral with regard to jurisdictional claims in published maps and institutional affiliations.